Wood Sci Technol
DOI 10.1007/s00226-014-0667-7

ORIGINAL

Impacts of fiber orientation and milling on observed crystallinity in jack pine

Umesh P. Agarwal · Sally A. Ralph · Richard S. Reiner · Roderquita K. Moore · Carlos Baez

Received: 6 February 2014
© Springer-Verlag Berlin Heidelberg (outside the USA) 2014

Abstract Influences of fiber orientation and milling on wood cellulose crystallinity were studied using jack pine wood. The fiber orientation effects were measured by sampling rectangular wood blocks in radial, tangential, and cross-sectional orientations. The influence of milling was studied by analyzing the unsieved and sieved milled wood fractions (all <1,000 µm). Fiber orientation effect was manifested in both X-ray and Raman measurements and was dependent upon the orientation of the sampled wood blocks. In Raman, the observed crystallinity was similar between the blocks sampled on the tangential and the radial faces. However, the estimated values were 5.5 % lower compared to that measured in a powdered sample pellet. Moreover, in these sampling modes, the orientation of the block with respect to the direction of the electric vector of the laser made a difference only for the tangential mode of sampling. When a wood block was sampled on the cross-sectional face, the observed Raman crystallinity was 3.9 % higher from that of the pellet. The observed crystallinity did not significantly differ with change in sample orientation with respect to the electric vector direction. In contrast, the Segal-WAXS study of the blocks indicated that compared to the pellet, the estimated crystallinities in the radial, tangential, and cross-sectional sampling modes were 5, 2, and 11 % lower, respectively. This suggested that the radial and the tangential faces of the blocks can be used to estimate the crystallinity of wood. With regard to the effect of milling on Raman and Segal-WAXS estimates, the wood crystallinity did not depend upon the particle sizes of the fractionated samples and was similar to that of the original unfractionated ground wood.

U. P. Agarwal (✉) · S. A. Ralph · R. S. Reiner · R. K. Moore · C. Baez
Forest Products Laboratory, USDA Forest Service,
One Gifford Pinchot Drive, Madison, WI 53726-2398, USA
e-mail:uagarwal@fs.fed.us

Published online: 05 September 2014

Introduction

In the utilization of wood and wood fiber, cell wall crystallinity is an important factor because it influences the physical and chemical behavior of these materials. For instance, crystallinity of the cellulose microfibrils controls the mechanical properties of wood (Murphey 1963; El-Osta and Wellwood 1972). Similarly, substrate crystallinity is an important consideration in the conversion of woods to cellulose ethanol where its reduction is believed to result in less recalcitrant biomass (Fan et al. 1980; Hall et al. 2010). Therefore, an accurate estimation of the crystallinity of wood and wood fibers is extremely valuable.

Cellulose crystallinity of woods can be determined using a number of analytical techniques, such as X-ray diffraction (Andersson et al. 2003; Leppänen et al. 2009), NMR (Newman and Hemmingson 1990; Newman 1999), Raman (Agarwal et al. 2013a), and sum frequency generation vibrational spectroscopy (Barnette et al. 2012). It is clear from the literature that various methods provide values of crystallinity that are different (Park et al. 2010). Additionally, most of the methods have limitations because they are not able to correctly account for the presence of amorphous cellulose or the contributions of the non-cellulosic components (hemicelluloses and lignin; Park et al. 2010; Agarwal et al. 2010 Bonarski and Olek 2011). For example, three distinct XRD methods are proposed to remove the contribution of amorphous cellulose from the diffractogram of cellulose samples (Park et al. 2010). The situation is further complicated by the fact that no cellulose standards are available.

Recently, to estimate crystallinity, near-IR FT-Raman-based methods were developed by Agarwal's group Fiber and Chemical Sciences Research (Agarwal et al. 2010). Subsequently, using the univariate Raman method, the crystallinity of woods and other lignocelluloses was estimated (Agarwal et al. 2013a) and it was reported that with proper corrections for the contributions of syringyl lignin and hemicelluloses, the method generated accurate values of wood Crystallinity. In this context, it is important to note that compared to Segal-WAXS (Segal et al. 1959), the Raman estimate is usually lower because it is correlated with the 21-Segal-WAXS, where 21 designates the 28 where amorphous contribution was measured (and subtracted) (Agarwal et al. 2010).

Then, there is the question of how fiber orientation in samples affects wood crystallinity. In the WAXS-based crystallinity determinations, wood has been sampled in various ways; for example, as a wood wafer (Andersson et al. 2003; Howell et al. 2011), wood chip (Barnette et al. 2012), and ground wood (Wellwood et al. 1974; Andersson et al. 2003; Agarwal et al. 2013a). Andersson et al. (2003) reported that for the investigated annual ring samples, the observed crystallinity from the tangential face was significantly higher compared to the ground wood where the fiber orientation was random. Although these researchers studied the thin tangential face, other wafer orientations and thicknesses were not studied. In view of this, the topic needs further investigation.

In the context of the Raman method, thus far, the crystallinity has always been measured using ground wood, and therefore, it would be of interest to find out how sampling solid wood on its various faces affects the crystallinity estimate. It is

hoped that understanding sampling effects could eventually open the door to more sampling options.

On the other hand, sampling wood post-milling entails the risk that the crystallinity may be modified. Therefore, it was decided to address the issue of crystallinity change upon milling of wood because to the best of the authors' knowledge this topic has not received much attention. Moreover, in an earlier research by the authors on effects of crystallinity and delignification on enzyme hydrolysis, it was observed that smaller size fractions had lower crystallinity values as determined by Raman (Agarwal et al. 2013b). Therefore, to study crystallinity change upon milling, unsieved and sieved milled wood fractions were studied. The reasoning behind this approach was that smaller fiber particles, present in lower sized fractions, are likely to have undergone a higher level of mechanical degradation because they are generated as a result of an increased degree of milling.

The objective of this investigation was to evaluate how Segal-WAXS and FT-Raman-determined crystallinities of jack pine are affected by sampling wood in different ways; specifically, wood blocks in different orientations and the pellets of unsieved and sieved fractions of milled wood.

Materials and methods

Wood preparation

Blocks of wood

A part of the 48-year-old jack pine (*Pinus banksiana*) stem was used to make ½- × ½- × 1-cm-small rectangular blocks (each block had six sides or faces). Three blocks of sapwood and two blocks of heartwood were used in this study. Only heartwood contained juvenile wood and no compression wood was present in any of the samples used in this study. However, both early wood and late wood were present in the blocks.

Milled wood and its fractions

Jack pine heartwood and sapwood chips were ground to pass a 1-mm (1,000-μm) screen in a Wiley mill. A series of US Standard Testing sieves were used to separate the wood meal into various size fractions. An initial sieving using a stack of three sieves was done for 25 min on a mechanical shaker with a hammer rap. The sample integrity for each sieve pan fraction was then checked by additional shaking until the residue in the receiving pan was minimal. The first number in the pair for the fraction designation is the size of the sieve aperture that retains the wood meal, and the second number is the size of the sieve through which the material has passed. The following eight size fractions were prepared 590–1,000, 420–590, 250-420, 177–250, 149–177, 74–149, 53–74, and <53 μm. The first three sieve fractions contained about 90 % of the wood meal.

Solvent extraction

Wood blocks

The wood blocks were extracted with 9:1 acetone–water and 2:1 toluene–95% ethanol under vacuum (25 psi) for 30 min. The blocks were put in the solvent mixture and vacuum was started. After 30 min, all blocks were completely submerged and the vacuum was repeated twice for each extraction-solvent mixture.

Particle sizes

Prior to fractionation, the ground wood was extracted by percolation with 9:1 acetone–water until the yields of extractives were minimal. The extracted wood meal was then air-dried. A high level of background fluorescence (upon laser excitation), more noticeable in the smaller-sized fractions, was reduced in part by additional extraction of the wood meal fractions. The fractions were each stirred for 2 h in acetone–water (9:1) followed by filtration, and the procedure was repeated two more times.

Acid chlorite delignification

Acid chlorite treatment of the 420–590 and <53-μm milled wood fractions was carried out by using the recommended procedure (Browning 1967). The fractions were each suspended in water at about 70 °C, and then glacial acetic acid and sodium chlorite were added. Over 7 h, three additional charges of chemicals were added.

Near-IR FT-Raman

All samples were analyzed with a Bruker MultiRam spectrometer (Bruker Instruments Inc., Billerica, MA, USA). This Raman system is equipped with a 1,064-nm 1,000-mW continuous-wave diode-pumped Nd:YAG laser. The wood blocks were analyzed in various orientations as shown in Fig. 1. For the ground wood, spectra were obtained from pellets that were made from ~ 150 mg of wood meal, Each pellet was ~9 mm in diameter and 1–2 mm in thickness. The wood meal was pressed in a steel die using a Fred Carver Laboratory Press and ~ 270×10^6 dyn/cm^2 of pressure. The laser power used for sample excitation was between 300 and 600 mW, and 1,024 scans were accumulated. Bruker's OPUS software program was used to find peak positions and process the spectral data. The processing of the spectra included, among other things, selecting a specific spectral region, baseline correction, and normalization.

X-ray diffraction

Wide-angle X-ray diffraction profiles in the reflection mode were recorded on a Bruker D8 Discover diffractometer with monochromatic CuKα (wavelength 1.5418) point source and a VÅNTEC-500 detector at the Materials Research Science and Engineering Center, University of Wisconsin, Madison. The beam aperture of 0.5 mm was used. In all cases, diffractograms were obtained on the same samples

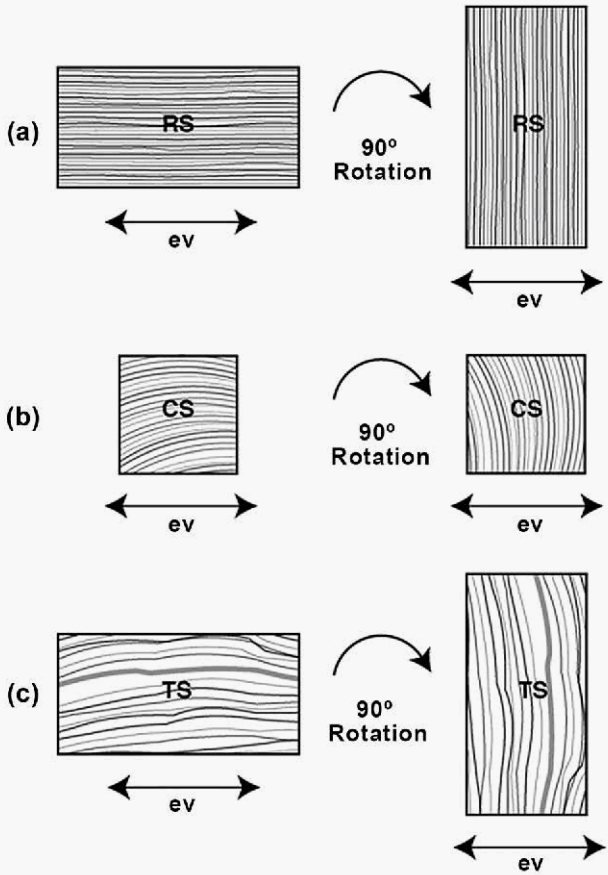

Fig. 1 Sampling orientations of wood blocks in Raman: **a** radial, **b** cross-sectional, and **c** tangential. In all cases, after sampling in the *left side* geometry, the blocks were rotated in the plane by 90° and re-analyzed in the rotated orientation. *ev* electric vector direction of the laser light

that were previously analyzed in FT-Raman. In WAXS, both sides of a particular face were sampled; i.e., a total of 10 diffractograms of each of the radial, tangential, and cross-sectional face. For example, the radial face diffractograms consisted of four heartwood and six sapwood samplings (from two heartwood and three sapwood blocks, respectively).

Crystallinity calculation

Raman

Using the previously established correlations (Agarwal et al. 2010, 2013a), which were based on the Bruker RFS-100 and MultiRam instruments, the univariate Raman crystallinities (X) were estimated. Based on RFS-100, Eq. (1) was developed for estimating the Raman crystallinity (Agarwal et al. 2010), and because MultiRam

was used in the present investigation, the inter-instrument calibration correction (RFS-100 vs. MultiRam) was carried out using Eq. (2) to get the RFS-100 equivalent crystallinity ($X_{RFS-100}$).

$$X_{\mathrm{MultiRam}} = ((I_{380}/I_{1096}) - 0.0286)/0.0065 \tag{1}$$

$$X_{\mathrm{RFS-100}} = (X_{\mathrm{MultiRam}} + 2.0212)/0.8222 \tag{2}$$

Additionally, the sample spectra were corrected for change in the response of the MultiRam optics over time. Using the white light in the sample compartment, the "reference correction" was performed on each sample spectrum. The estimated Raman crystallinities are also corrected for the hemicelluloses contributions (Agarwal et al. 2013a). No syringyl lignin correction is required (Agarwal et al. 2013a) because jack pine is a conifer with minimal syringyl lignin.

The standard deviation (SD) listed is based on three spectra from each sample that were obtained from two different pellets. Two spectra per pellet were acquired by changing the side that was exposed to the laser.

WAXS

For each of the samples, WAXS crystallinity was calculated by subtracting the amorphous contribution approximately at $2\theta = 18°$ ($100 \times (I_{22.5} - I_{18})/I_{22.5}$; called Segal-WAXS). This was done after a straight line was drawn between the lowest intensity points in the 2θ range of 7° and 37°. This method is also known as the [002] peak height ratio method (park et al. 2010).

ANOVA and paired *t* tests

One-way ANOVA was used to determine whether there were statistically significant differences between the observed Raman crystallinity of wood blocks in various sampling geometries.

To determine whether different orientations of electric vector or the wood block influenced Raman crystallinity measurements, paired *t* tests were used to compare the observed crystallinity of each block of wood when measured in different ways. The criteria for statistically significant was $p \leq 0.05$.

Results and discussion

Crystallinity of blocks

In the following, it is assumed that the observed crystallinity differences of the blocks in both the Raman and Segal-WAXS methods are not due to the presence of varying amounts of early wood and late wood in the samples. This assumption is based on the literature report that showed that the crystallinity of early wood and late wood is similar (Newman 2005).

Raman

The orientations in which the sapwood and heartwood blocks were sampled in Raman are shown in Fig. 1. These modes consisted of sampling at the (a) radial, (b) cross-sectional, and (c) tangential faces. In all cases, after sampling in the left side geometry (Fig. 1), the block was rotated, in plane, by 90" and analyzed in the rotated orientation. This was carried out because band intensities in oriented fibers depend upon polarization of the exciting light relative to the orientation of the cellulose molecules (Wiley and Atalla 1987). Average spectra of heartwood blocks obtained in (a), (b), and (c) sampling modes are shown in Fig. 2. The spectra were obtained such that the sample orientation relative to the electric vector of the laser was horizontal (defined in Table 1). Figure 2 spectra are normalized using 1,096 cm^{-1} band in the spectrum. Among the spectra, 380 cm^{-1} peak has higher intensity for the sampling in the cross-sectional mode. Moreover, in this mode, many other bands at higher wave numbers were sharper and more intense (only a limited region is shown in Fig. 2). In a cellulose spectrum, the latter features imply higher crystallinity (Agarwal et al. 2010) or orientation effects (Wiley and Atalla 1987). Considering that the crystallinity estimation in Raman is directly proportional, the intensity ratio I_{380}/I_{1096} (Eq. 1) indicated that the observed crystallinity was higher compared to the other two modes. Cellulose crystallinity calculation results are listed in Table 1.

The data indicated the following: For a given orientation, the observed crystallinity between heartwood and sapwood was only slightly different, indicating that crystallinity was similar between heartwood and sapwood—a result that has been previously reported for white oak and pacific yew (hardwood and softwood, respectively; Agarwal et al. 2013a). Another observation was that within a given "face" of sampling (i.e., Fig. 1a, b, or c), different sample orientations with respect to the electric vector gave the same value of crystallinity (Table 1, horizontal and vertical data sets). This indifference was expected for the cross-sectional sampling but not for the longitudinal mode of sampling. Nevertheless, the latter may be because, in the horizontal and vertical arrangements, although tracheid fibers are oriented differently with regard to the electric vector direction, the Raman intensity anisotropy is likely to be minimized due to multiple reflections and refractions of Raman-scattered photons at the solid surfaces of the sample.

When the cross-sectional crystallinity estimates are compared with those obtained in the longitudinal modes (radial and tangential), the data in Table 1 show that the observed crystallinities were 8.4 % higher in the former mode (average crystallinities 59.1 vs. 50.7 % for cross-sectional and longitudinal modes, respectively). This compares to the reported jack pine Raman crystallinity of 55.3 % (Agarwal et al. 2013a) obtained using the ground wood. Compared to the observed crystallinity in longitudinal modes, higher crystallinity in cross-sectional mode is likely to arise from the fact that in the latter mode, the intensity ratio 380/1096 is significantly higher. This is because the angle between the electric vector of the laser and the fiber axis is close to 90" (Wiley and Atalla 1987).

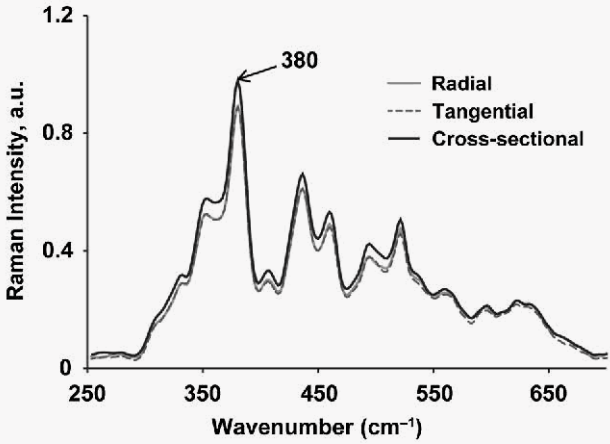

Fig. 2 Comparison of Raman peak intensity at 380 cm^{-1} as a function of radial, tangential, and cross-sectional sampling modes

ANOVA analysis

One-way ANOVA of the data in Table 1 shows statistically significant difference in the crystallinity data ($F(11,24) = 12.89$, $p = 0.0000$). However, when the analysis was carried out on the subset that excluded the cross-sectional data, the results were ($F(7,16) = 3.173$, $p = 0.026$). The p value was lower than 0.05 implying slight significance, but it was not that much farther apart.

Paired t tests

Vertical versus horizontal vector The vertical and horizontal vectors did give statistically significant different crystallinity measures ($p \leq 0.05$) in both heartwood and sapwood in the tangential orientation, but not in the radial or transverse orientation.

Impact of different sides on measured crystallinity The horizontal and vertical vector data were pooled to yield six data points per condition. The paired t test results showed that the transverse orientation gives a different crystallinity reading than the radial or tangential face, which were indistinguishable from each other. Heartwood and sapwood gave the same result.

Segal-WAXS

Because "horizontal" and "vertical" terminology is meaningless in WAXS, the same data are shown in both the cells in Table 1. Average diffractogams of heartwood blocks obtained in radial, tangential, and cross-sectional sampling modes are shown in Fig. 3. Of the three modes of sampling, highest crystallinity was obtained for the tangential mode (79.2, 75.4, and 69.6 % for tangential, radial, and cross-sectional modes, respectively). This compares with the value of 76.5 %

Table 1 Cellulose crystallinity of jack pine blocks

Sample orientation relative to electric vector	% Crystallinity, heartwood ± SD		% Crystallinity, sapwood ± SD	
	Raman	Segal-WAXS[b]	Raman	Segal-WAXS
Radial				
Horizontal[a]	53.1 ± 3.6	75.4 ± 2.2	52.7 ± 3.3	69.9 ± 6.5
Vertical	49.3 ± 0.4	75.4 ± 2.2	48.4 ± 1.5	69.9 ± 6.5
Tangential				
Horizontal	53.3 ± 1.1	79.2 ± 3.6	50.1 ± 2.0	70.7 ± 5.2
Vertical	50.7 ± 0.9	79.2 ± 3.6	47.9 ± 1.6	70.7 ± 5.2
Cross-sectional				
Horizontal	58.4 ± 1.1	69.6 ± 4.5	58.4 ± 3.0	66.3 ± 9.9
Vertical	59.6 ± 2.6	69.6 ± 4.5	59.9 ± 2.4	66.3 ± 9.9

[a] Grain direction parallel to

[b] Horizontal or vertical terminology not applicable in WAXS; same crystallinity values are shown in both cells

obtained from the unfractionated ground wood (<1,000 µm). Or in other words, compared to the pellet the estimated crystallinities in the tangential mode were higher by 3.5 %, whereas both the radial and cross-sectional sampling modes gave lower values, 1.4 and 9 %, respectively. The higher crystallinity in tangential mode is supported by the finding of Andersson et al. (2003), who have reported that for Norway spruce the estimated crystallinity of the 1-mm-thick tangential wood wafer was significantly higher compared to the ground wood. In the current study, the observed increase in crystallinity was rather limited and this may have to do with the difference between the sample thicknesses and the fibril angles between the two studies. The tangential samples in this study were five times thicker.

Compared to heartwood blocks, the crystallinities of sapwood blocks were somewhat lower (Table 1, lower by 12–5%). In addition, the heartwood, tangential, and radial blocks provided crystallinity closer to ground wood pellet (Table 2, 76.5 %), and in these modes, the WAXS crystallinity estimates were minimally influenced by fiber orientation [Segal-crystallinity for the heartwood tangential and radial modes was 79.2 and 75.4 %, respectively (Table 1)].

Paired t tests

Within heartwood and sapwood sample sets, the crystallinities obtained in different modes (tangential, radial, and cross-sectional) were compared. Except for the heartwood pair tangential–cross-sectional, the values were found to be not significantly different.

Although in both Raman and Segal-WAXS, compared to the crystallinity of the ground wood, there are some differences in the crystallinity of blocks, the blocks can be used to evaluate relative crystallinity and changes in relative crystallinity. This is true as long as the composition of wood and sampling orientation do not change. If that is not the case, more caution needs to be exercised because, in both the methods, sample composition plays a role (Agarwal et al. 2013a).

Crystallinity of ground wood fractions

Raman

For the various sized fractions, the Raman method-based crystallinity estimations are listed in Table 2. Here, Raman-estimated crystallinities of two delignified fractions (420–590and <53 µm) are also reported. The spectra are shown in Fig. 4, and the crystallinity data are plotted in Fig. 5. As expected, in Table 2, the Raman crystallinities are lower compared to the Segal-WAXS values. The latter has to do with how the two measurements are correlated (Agarwal et al. 2013a). Except for the <53 µm fraction, the crystallinities between the fractions were similar and milling did not have an impact. Based on the 2-tailed *t* test, the crystallinity of the <53 µm fraction was indeed distinct from the values of the other fractions.

Considering that the fluorescence in the Raman spectrum of the <53 µm fraction was significantly higher compared to other fractions (not seen from Fig. 4 because the background was subtracted), it was possible that the former impacted the Raman

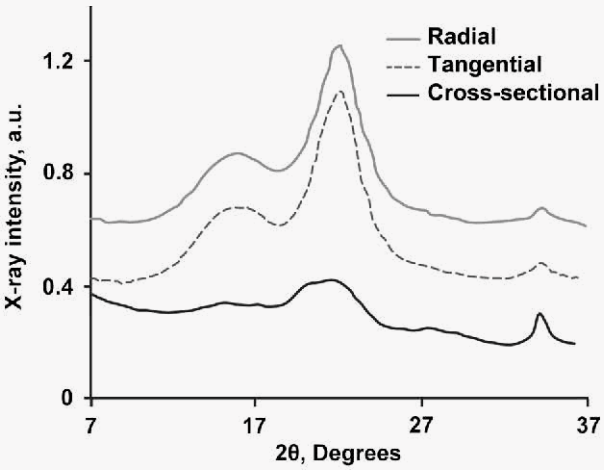

Fig. 3 Comparison of WAXS diffractograms in radial, tangential, and cross-sectional sampling modes

Table 2 Average crystallinity of milled wood fractions

Particle size, range	% Raman crystallinity, ±SD	% Segal-WAXS crystallinity, ±SD
Ground wood (<1,000 μm)	55.3 ± 1.9	76.5 ± 0.5
590–1,000 μm	49.6 ± 1.4	76.9 ± 2.5
420–590 μm	46.9 ± 1.0	80.4 ± 1.1
250–420 μm	50.7 ± 0.3	81.0 ± 1.1
177–250 μm	49.6 ± 0.9	80.3 ± 1.2
149–177 μm	52.6 ± 0.4	81.3 ± 2.8
74–149 μm	53.3 ± 2.0	79.7 ± 0.2
53–74 μm	53.5 ± 2.1	80.1 ± 0.2
< 53 μm	39.3 ± 1.1	81.0 ± 0.9
Delignified; 420–590 μm	58.8[a] ± 2.3	ND[b]
Delignified; <53 μm	56.1[a] ± 0.8	ND

[a] Crystallinity estimation is higher due to fluorescence reduction upon delignification

[b] Not determined

estimation of crystallinity. Previously (Agarwal et al. 2013a), in the case of most softwoods, the influence of sample fluorescence on crystallinity estimation by Raman was found to be small provided that the sample fluorescence was low. However, in cases where the latter contributed significantly, the crystallinity data depended upon how the fluorescence signal impacted the intensities of the bands involved in the crystallinity estimation (Eq. 1; namely 1,096 and 380 cm^{-1} bands). Nevertheless, irrespective of the presence of the fluorescence, the nature of the qualitative information in the spectra remains the same. In view of this, to minimize the influence of fluorescence in the spectrum of <53 μm fraction, this fraction and 420–590-μm sieved fraction (as control) were acid chlorite delignified and the

crystallinities were re-estimated (also reported in Table 2). The treatment by acid chlorite was used which is a well-known method to remove lignin. Upon delignification, Klason lignin value dropped from about 30.7 % (similar in both the fractions) to 1.6 and 1.3 % for 420–590 and <53 µm delignified fractions, respectively. Moreover, it is known that in Raman spectroscopy, lignin is primarily responsible for laser-induced fluorescence (Agarwal 1999). The crystallinity of the delignified fractions in Table 2 is similar but higher (significantly higher for the <53 µm case) compared to the corresponding non-delignified fractions. This is expected because compared to the 1,096 cm^{-1} region, more fluorescence was removed from the 380 cm^{-1} region. Earlier work by the authors has shown that an accurate estimation of the cellulose crystallinity can be obtained from the Raman spectrum where the contribution of sample fluorescence has been mostly removed (Agarwal et al. 2013a). Therefore, when the "fluorescence factor" is taken into account, the Raman crystallinity of the <53 µm fraction was also similar to that of

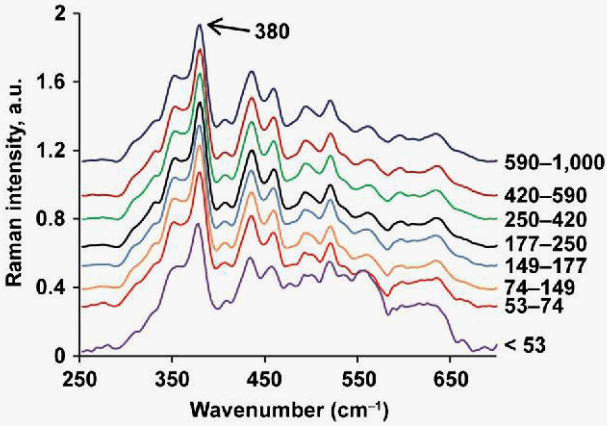

Fig. 4 Comparison of Raman peak intensity at 380 cm^{-1} in the normalized spectra of various sieved fractions. The sieved fractions are annotated in µm

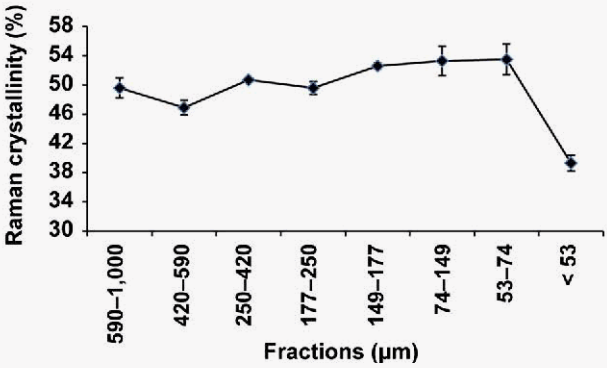

Fig. 5 Raman crystallinity of different sire fractions of ground wood

the other larger size fractions (however, it ought to be noted that Fig. 5 shows only the crystallinity of the non-delignified fraction). In light of this finding, the earlier reported result (Agarwal et al. 2013b) seems to be in error where smaller wood particles were reported to have lower crystallinity. The reason for the erroneous result seems to be the level of fluorescence from the smaller size particles. In Table 2, Segal-WAXS crystallinities for the two delignified fractions are not reported because the presence of sample fluorescence is not an issue in X-ray diffraction.

Segal-WAXS

For the different fractions, the Segal-WAXS estimates of crystallinities are reported in Table 2. The average diffractograms are shown in Fig. 6 and the crystallinity data

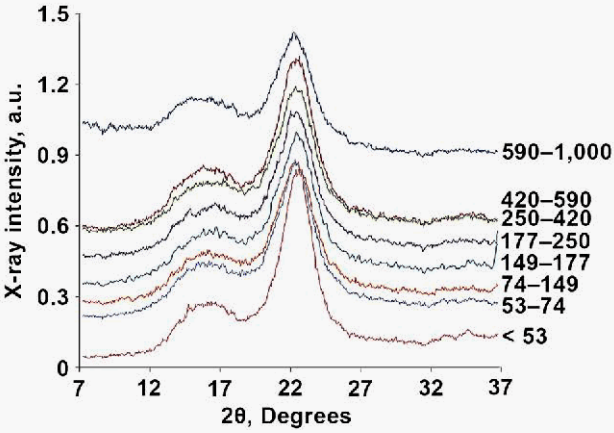

Fig. 6 Comparison of WAXS diffractograms of various sieved fractions. The sieved fractions are annotated in µm

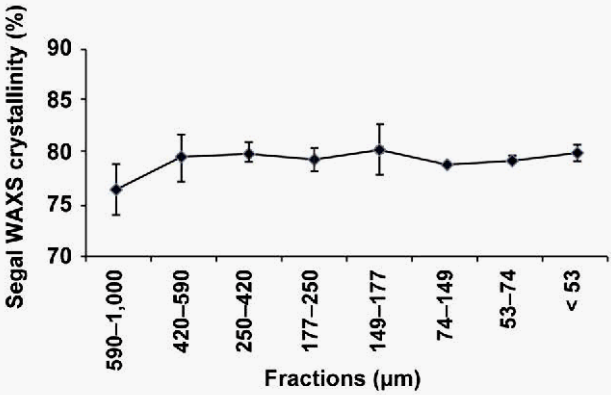

Fig. 7 Segal-WAXS crystallinity of different sire fractions of ground wood

are plotted in Fig. 7. Based on Table 2 and Fig. 7, it is clear that there is no significant change in the cellulose crystallinity. This further supported the finding above that was obtained using the FT-Raman method.

Conclusion

Cellulose crystallinity of jack pine was estimated using small rectangular blocks of wood and by fractionating the ground wood into various fractions. Near-IR FT-Raman and Segal-WAXS methods were used to measure the Crystallinity. It was found that if the wood blocks are used, the error in crystallinity estimation compared to that of a milled wood pellet depended upon the blocks orientation and the method used in the assessment. On the other hand, for the investigated size fractions of the ground wood, both Raman and Segal-WAXS indicated that the mechanical processing by milling did not change the cellulose crystallinity of jack pine.

References

Agarwal UP (1999) An overview of Raman spectroscopy as applied to lignocellulosic materials. In: Argyropoulos DS (ed) Advances in lignocellulosics characterization. TAPPI Press, Atlanta, pp 209–225

Agarwal UP, Reiner RS, Ralph SA (2010) Cellulose I crystallinity determination using FT-Raman spectroscopy: univariate and multivariate methods. Cellulose 17:721–733

Agarwal UP, Reiner RS, Ralph SA (2013a) Estimation of cellulose crystallinity of lignocelluloses using near-IR FT-Raman spectroscopy and comparison of the Raman and Segal-WAXS methods. J Agric Food Chem 61:103–113

Agarwal UP, Zhu JY, Ralph SA (2013b) Enzymatic hydrolysis of loblolly pine: effects of cellulose crystallinity and delignification. Holzforschung 67:371–377

Andersson S, Serimaa R, Paakkari T, Saranpaa P, Pesonen E (2003) Crystallinity of wood and the sire of cellulose crystallites in Norway spruce (*Picea abies*). J Wood Sci 49:531–537

Barnette AL, Lee C, Bradley LC, Schreiner EP, Park YB, Shin H, Cosgrove DJ, Park S, Kima SH (2012) Quantification of crystalline cellulose in lignocellulosic biomass using sum frequency generation (SFG) vibration spectroscopy and comparison with other analytical methods. Carbohydr Polym 89:802–809

Bonarski J, Olek W (2011) Application of the crystalline volume fraction for characterizing the ultrastructural organization of wood. Cellulose 18:223–235

Browning BL (1967) Methods of wood chemistry, vol II. Wiley-Interscience, New York

El-Osta MJM, Wellwood RW (1972) Short-term creep as related to cell-wall crystallinity. Wood Fiber Sci 4:204–211

Fan LT, Lee Y-H, Beardmore DH (1980) Mechanism of the enzymatic hydrolysis of cellulose: effects of major structural features of cellulose on enzymatic hydrolysis. Biotechnol Bioeng 22:177–199

Hall M, Bansal P, Lee JH, Realff MJ, Bommarius AS (2010) Cellulose crystallinity—a key predictor of the enzymatic hydrolysis rate. FEBS J 277:1571–1582

Howell C, Hastrup ACS, Jara R, Larsen HF, Goodell B, Jellison J (2011) Effects of hot water extraction and fungal decay on wood crystalline cellulose structure. Cellulose 18:1179–1190

Leppänen K, Andersson S, Torkkeli M, Knaapila M, Kotelnikova N, Serimaa R (2009) Structure of cellulose and microcrystalline cellulose from various wood species, cotton and flax studied by X-ray scattering. Cellulose 16:999–1015

Murphey WK (1963) Cell-wall crystallinity as a function of tensile strain. For Prod J 13:151–155

Newman RH (1999) Estimation of the lateral dimensions of cellulose crystallites using 13C NMR signal strengths. Solid State Nucl Magn Reson 15:21–29

Newman RH (2005) Homogeneity in cellulose crystallinity between samples of *Pinus radiata* wood. Holzforschung 58:91–96

Newman RH, Hemmingson JA (1990) Determination of the degree of cellulose crystallinity in wood by carbon-I3 nuclear magnetic resonance spectroscopy. Holzforschung 44:351–355

Park S, Baker JO, Himmel ME, Parilla PA, Johnson DK (2010) Cellulose crystallinity index: measurement technique and their impact on interpreting cellulose data. Biotechnol Biofuels 3:10

Segal L, Creely JJ, Martin AE, Conrad CM (1959) An empirical method for estimating the degree of crystallinity of native cellulose using the X-ray diffractometer. Text Res J 29:786–794

Wellwood RW, Sastry CBR, Micko MM, Paszner L (1974) On some possible specific gravity, holo- and α-cellulose, tracheid weight/length and cellulose crystallinity relationships in a 500-year-old Douglas-fir tree. Holzforschung 28:91–94

Wiley JH, Atalla RH (1987) Raman spectra of celluloses. In: Atalla RH (ed) The structures of cellulose, ACS symposium series, vol 340. ACS, Washington DC, pp 151–168